applied sciences

MDPI

Article

Applications of Electrical Resistivity Surveys in Solving Selected Geotechnical and Environmental Problems

Mariusz Lech *, Zdzisław Skutnik, Marek Bajda and Katarzyna Markowska-Lech

Faculty of Civil and Environmental Engineering, Warsaw University of Life Sciences, 02-787 Warsaw, Poland; zdzislaw_skutnik@sggw.pl (Z.S.); marek_bajda@sggw.pl (M.B.); katarzyna_markowska_lech@sggw.pl (K.M.-L.)

* Correspondence: mariusz_lech@sggw.pl; Tel.: +48-22-593-5201

Received: 12 February 2020; Accepted: 18 March 2020; Published: 26 March 2020

Abstract: Standard test methods may not be suitable or sufficient for determining the geotechnical conditions of a structure's subsoil and the effects of the designed structures on the environment. Geophysical test methods, validated with other methods, may prove useful. In recent years they have found many new applications in engineering practice, both geotechnical and environmental. The advantages of geophysical methods include the non-destructive and non-invasive nature of the tests, their low costs and quick results, as well as compatibility with different materials, including soils, solid rocks, wastes and anthropogenic formations. The paper presents the analysis of laboratory and field investigations including research in a modified oedometer, resistivity chamber, electrical resistivity tomography (ERT) and resistivity cone penetration test (RCPT). Laboratory tests allowed for the assessment of the degree of saturation and porosity of sandy and clayey soils. The tests were carried out on saturated and unsaturated soil samples and allowed for the determination of some relationships between electrical conductivity and porosity. The proposed equations were used to assess parameters in in situ studies using RCPT tests and showed good agreement with reference values based on undisturbed soil samples. ERT tests confirmed the usefulness of electrical measurements in the quality assurance of subsoil and hydrotechnical structures. The tests showed weakening zones in the levee body, discontinuity of the vertical sealing system on the modernized section of the embankment, and location of the top of clay deposits.

Keywords: electrical resistivity measurements; RCPT; oedometer tests; electrical resistivity chamber; saturation degree; porosity

1. Introduction

Geophysical methods have been used for many years in prospecting for industrial and energy resources, geological and engineering surveys, as well as geotechnical surveys. Electrical resistivity, electromagnetic and seismic methods are commonly used in practical and research applications which include: geological [1–4] and hydrogeological [5–7] investigations of the subsoil, technical conditions of hydrotechnical structures and other civil engineering structures [8–11], testing of porosity [12–17], moisture content [18,19] and saturation degree [12,15,20,21] of the subsoil, as well as monitoring of landfills, and agricultural and post-industrial areas [22–26].

A geophysical survey comprises the measurement of physical properties, usually at the ground surface level without disturbing the soil structure, followed by comprehensive processing and interpretation of the recorded data to gather information on the soil type and structure. Its advantages include a non-invasive nature, low costs and quick results, as well as an ability to create a spatial subsoil model without the use of heavy equipment. One of the methods used for many years in subsoil

investigations is electrical resistivity tomography. The method is based on the assumption that soil and rocks, as well as other materials, conduct electricity. As shown by previous studies [12,15,19,21,27], the method is affected by the soil moisture content and water saturation, its porosity and contamination level of water in the soil pores, in particular with salt [15,28,29] and NAPL (non-aqueous phase liquid) compounds [19,30], and change of stress conditions [8,16].

Extensive development of survey methods in the recent years, both in geophysics and geotechnics, has allowed for the modification of the existing measuring instruments. New instruments have been developed, including the RCPTU (resistivity cone penetration test with pore pressure "u" measurements) probe [30–32], for measuring electrical resistivity and other common parameters. These tests are mostly used in geotechnics to assess the condition of, e.g., a structure's foundation [33,34], hydrogeological conditions [35,36] or physico-mechanical properties of the soil [37].

Since the electrical resistivity of some minerals (e.g., quartz and silica minerals) is high and the soil skeleton plays the role of an isolator, the electric current flows through the soil voids filled with water. In coarse grained materials the results of resistivity tests may be significantly affected by water mineralization, and its saturation degree and porosity. If the water content (saturation degree) is constant, soil resistivity generally becomes a function of salts dissolved in the soil water solution and soil porosity. The principal empirical equations concerning relationships between soil resistivity and its physical parameters were presented by Archie [12] and others [2,10,18,21,38]. In most porous and clay-free materials, the resistivity of the saturated material may be described as:

$$\rho_{bSAT} = \rho_f \cdot F = \rho_f \cdot a \cdot n^{-m}, \quad (1)$$

where ρ_{bSAT} is thelectrical resistivity of soil in fully saturated conditions [Ω·m], ρ_f is the electrical resistivity of fluid in pore spaces [Ω·m], F is the formation factor [-], n is the porosity [-], and a and m are the empirical constants (depending on pore shape and cementation).

In soils containing clay minerals a double layer phenomenon, which introduces an additional conductivity called surface conductance to the system [17,39], should additionally be considered. Surface conductance is a special form of ionic transport occurring at the interface between the solid and fluid phases of the system. In clayey materials, the resistivity may be expressed as:

$$\rho_{bSAT} = \frac{\rho_f \cdot a \cdot n^{-m}}{1 + \rho_f \cdot B^+ \cdot Q_v}, \quad (2)$$

where B^+ is the equivalent ionic conductance of clay exchange cations [S·m^2/meq] and Q_v is the cation exchange capacity (CEC) per unit of pore volume [meq/m^3].

The first parameter, B^+, is a function of specific conductivity of the equilibrating electrolyte solution conductance, which describes how easily the cations can move along the clay surface. The cation exchange capacity defines the cation concentration (mainly Mg^{2+}, Na^+ and K^+) on the surface area and can be obtained in laboratory tests.

Measurements of soil electrical resistivity have been used to predict various soil parameters: porosity, degree of saturation, water content, degree of soil compaction, liquid and plastic limits, liquefaction potential, and others. It is one of the most widely used geophysical methods applied to solve geological, geotechnical, and environmental issues. The present study investigates the possibility to predict various soil conditions (e.g., soil saturation and compaction) and parameters detecting and locating failures of sealing systems, and to correlate electrical resistivity measurements with geotechnical data. The presented laboratory tests have established relationships between porosity, saturation degree and electrical resistivity in sands and clayey soils which were then applied in the field at the Stegny site and the SGGW Campus in Warsaw. In laboratory investigations, a unique test equipment designed for this purpose has been used. This study enabled to improve and confirm our understanding of subsurface studies with application of electrical resistivity measurements and selecting the correct approach when designing the scope of research for a specific case. The paper

presents several case studies employing electrical resistivity tomography and RCPT testing, aimed at presenting examples of practical use of electrical resistivity tests in environmental geotechnics. Hence, its applicability as a guide to the practical use of ERT for environmental geotechnics is important, providing a better discussion of the obtained results, opportunities and limitations of the methodology.

2. Materials and Methods

2.1. Characteristics of the Test Sites

The study area lies within a regional geomorphological unit known as the Warsaw Basin. All test sites are located in the Vistula River valley or in the vicinity of the valley (Figure 1). The first test site at Stegny is the place where a wide research program was executed by the Warsaw University of Life Sciences and the University of Warsaw during the last few years. The main purpose of these investigations was to estimate the physical properties and mechanical parameters of Pliocene clays. The Stegny site is located in the southern district of Warsaw. Its stratigraphy includes Quaternary deposits developed as fine and medium-dense sands of a thickness not exceeding 4.5 m, underlain by overconsolidated Pliocene clays. The free groundwater table was measured at a depth of 3.2 m.

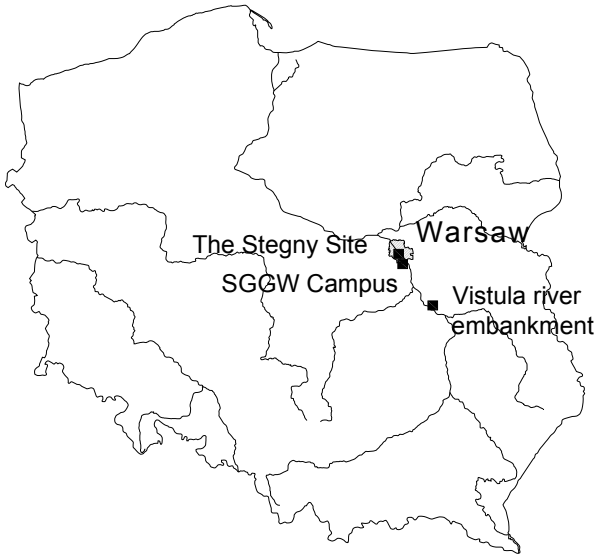

Figure 1. Location map of the test sites.

The second test site at the SGGW Campus covers an area in the margin of a denudated moraine plateau. The site is located in the marginal zone of the southern part of the Warsaw moraine upland in Ursynów district. Here, these sediments form a continuous, distinct layer, consisting mostly of fine sands. Above the fluvioglacial sediments lies a layer of melt-out sediments from the Odranian Glaciation, represented by Glacial till. In situ (boreholes, RCPTU tests) and laboratory investigations have allowed to conclude that the surface zone consists of overconsolidated sandy clays, grey and brown in color.

Figure 2 presents the grain-size distribution curves for several soil samples: fine and medium sands (FSa, MSa), and clays (Cl and siCl) taken from the subsoil of the Stegny site, and sandy clays (sisaCl) and clayey sands (clSa) taken from the SGGW Campus. The graph contains also the grain-size distribution curves that have been tested in the laboratory, including sandy clays (sisaCl) from the SGGW Campus tested in a modified oedometer and samples of fine, medium and coarse sands (FSa, MSa and CSa) tested in the column apparatus.

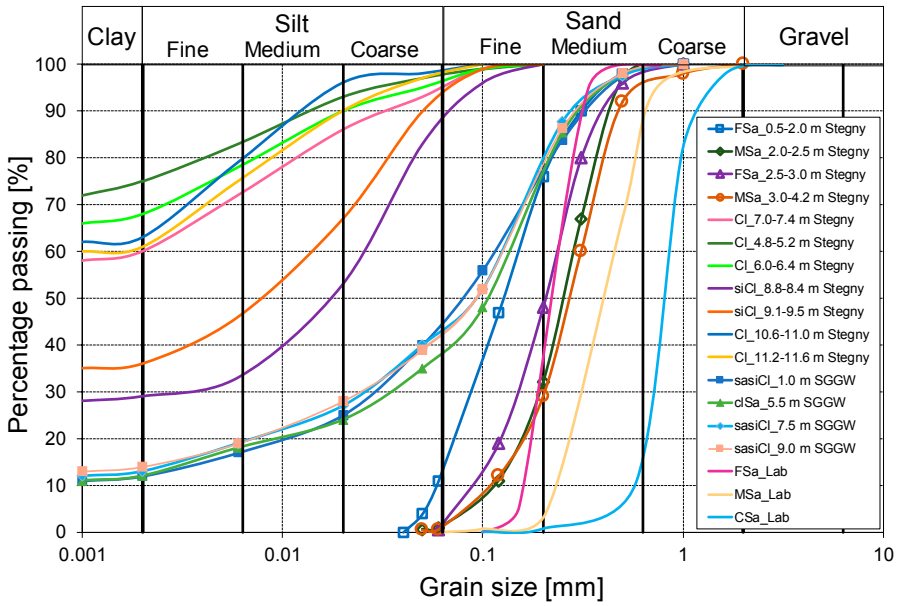

Figure 2. Grain-size distribution curves for soil samples taken directly from the test sites and assessed in the laboratory.

The last test site is the modernized right embankment of the Vistula River, located in the Maciejowicka Valley. Renovation works carried out in the recent years were enforced by numerous filtration deformations, which in extreme cases lead to instabilities. A section of the embankment examined before the modernization was built of locally available material, which was poorly graded fine and silty sands. Control tests using ERT and BAT–groundwater monitoring system, were carried out on selected sections of the flood embankment in which a diaphragm was installed.

2.2. In Situ Investigations

Theoretical foundations of the electrical resistivity method, widely used for the last 50 years, are well known [2,5,38]. In practice, the soil electrical resistivity is measured using a four-electrode configuration. In this method, an electrical current is supplied to the soil using two electrodes, inducing an electric field, whereas the other two measure its potential. Apparent electrical resistivity of the soil may be determined based on the known difference between the electric field potential (ΔV) and the current intensity (I) and the distance between the electrodes [38]. Apparent resistivity is expressed by the equation:

$$\rho_b = k\frac{\Delta V}{I}, \quad (3)$$

where ρ_b is the apparent resistivity [Ωm], I is the current applied to the soil by electrodes C1 and C2 [mA], V is the potential difference between electrodes P1 and P2 [mV], and k is the geometrical coefficient of electrode positioning [m].

Resistivity does not reflect properties of one particular soil type, but presents the capability for electrical conductivity of a subsoil located in the vicinity of a spatial electric field. Such resistivity is called apparent resistivity. The geoelectrical survey is based on the measurement of apparent resistivity accompanied with symmetrical rise of the distance between charged electrodes (current electrodes, C1 and C2). A wider distance between the electrodes results in deeper electric field penetration into the subsoil, which significantly influences the survey depth. For the purpose of the present study, electrical resistivity tomography (ERT) in the Wenner array was applied (Figure 3). A detailed description of this array and other complex configurations was published by Zahody et al. [5], Lowrie [38], Loke et al. [40], and Keller et al. [41].

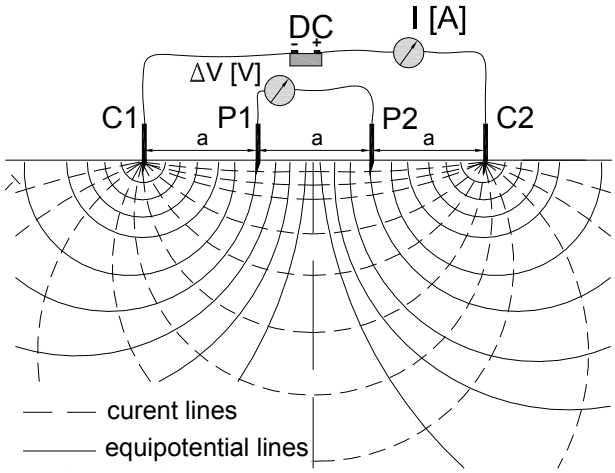

Figure 3. Four-electrode configuration for resistivity measurements, consisting of a pair of current electrodes (C1, C2) and a pair of potential electrodes (P1, P2).

The RCPT (RCPTU) cone (Figure 4) used to assess soil porosity, is a combination of a static CPTU (cone penetration test) probe with soil resistivity measurements. The probe consists of two main elements: first for measuring parameters determined in a standard CPTU test, and the second being an electrical resistivity measuring module. It includes two or four annular electrodes (at a spacing of 5 cm) with insulating plastic elements and an alternating current flowing between the electrodes.

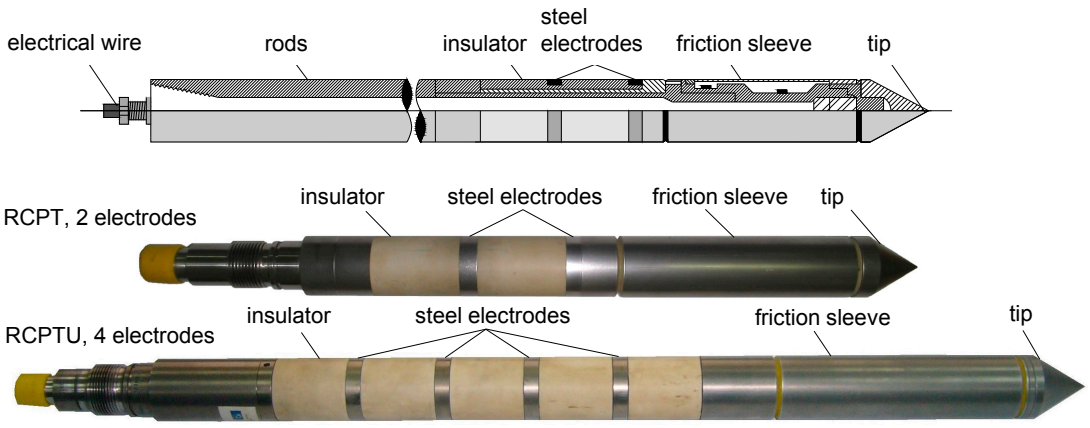

Figure 4. Cross-section and photographs of RCPT and RCPTU cones.

2.3. Laboratory Investigations

Two test stands adapted for testing non-cohesive and cohesive soils depending on the needs and the required scope of tests were installed in the laboratory. The column for testing non-cohesive soils was equipped with chemically insensitive graphite electrodes for measuring the electrical resistivity of sands and gravels (Figure 5).

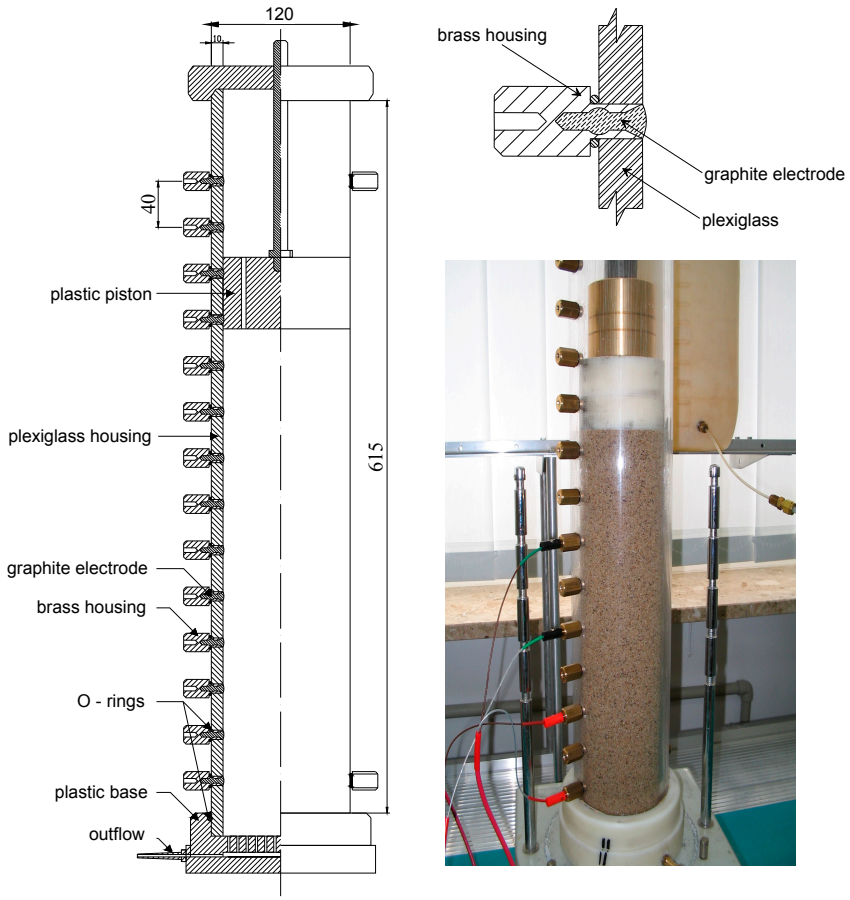

Figure 5. Column apparatus for measuring electrical resistivity of sands; scheme of apparatus and electrode and view of apparatus during sample preparation.

The column apparatus, in which the soil sample was placed, was made of materials that do not conduct electricity, and was embedded in a plastic base sealed with O-rings. One of the base elements was porous and connected to the column drainage system. A lid with a piston, which could move freely inside it and had two holes through which excess water could flow out of the sample, was installed in the upper part of the column. The installed electrodes (graphite electrodes at a spacing of 4 cm) allowed to control the variability of electrical conductivity at 3 levels of the soil sample. The column was calibrated using a potassium chloride solution with known electrical resistivity. Before testing, the soil was washed and dried, and then inserted in the measuring chamber in layers with a thickness of approximately 5 cm and compacted under a load of approximately 1 kN. A solution of potassium chloride with known electrical conductivity was supplied through an inlet in the bottom of the apparatus, which provided fully saturated conditions of the sample. The tests were also performed at not fully saturated conditions where soil with a different water content was then inserted.

The second test stand was a modified oedometer, in which electrodes were installed to register changes in the electrical resistivity of a sandy clay sample (sisaCl) taken from the SGGW Campus under load changes (Figure 6). The piston and oedometer ring, in which the soil sample was located, were made of an insulating material. Four flat copper ring electrodes were installed in the oedometer ring walls in a way that ensured the contact of the electrodes only with the soil sample and not with the brass casing. The width of the electrodes was 2.5 mm, while the inner diameter of the ring was 50 mm. The electrodes were arranged at equal, four-millimeter distances, in accordance with the four-electrode Wenner array (two outer electrodes were current electrodes generating the electric field in the soil sample, while the two inner electrodes in the ring were used to measure the electric field

potential). Before testing, the oedometer was calibrated using (potassium chloride) solutions with known electrical resistivity.

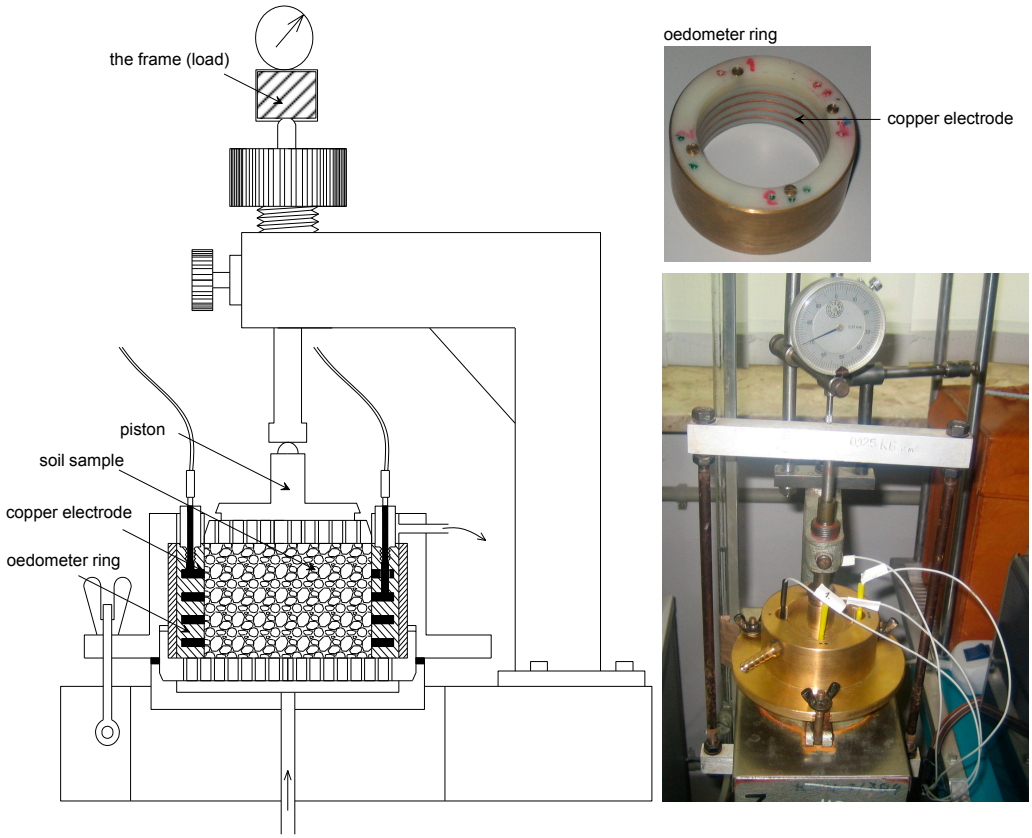

Figure 6. A modified oedometer for measuring electrical resistivity of clayey soils; scheme of apparatus and view of oedometer ring with electrodes and apparatus during the test.

3. Results and Discussion

3.1. Influence of Degree of Saturation and Porosity on Electrical Resistivity—Laboratory Investigations

Research in the column apparatus determined the impact of the degree of saturation and porosity on the electrical resistance of sandy soils. When assessing the impact of the degree of saturation vs. electrical resistivity, the soil samples had the relative density, D_r, in the range of 0.48 to 0.52, to ensure that the porosity of the material is relatively constant. The estimated relationship between the soil electrical resistivity and the saturation degree is:

$$S_r = \left(\frac{\rho_{bSAT}}{\rho_b}\right)^{\frac{1}{\beta}}, \quad (4)$$

here S_r is the saturation degree [-], ρ_{bSAT} is the electrical resistivity of soil in fully saturated conditions [Ω·m], ρ_b is the electrical resistivity of material/soil [Ω·m], and β is the empirical constant.

The empirical constants used in this equation and depending on the grain size of sand are shown in Table 1. It should be noted that the saturation exponent β is often adopted. The saturation exponent β most often occurs in the literature in the value range of 1.00 ÷ 2.50 [42,43]. At the same time, it should be mentioned that hysteresis occurs during sample saturation and desaturation processes and is influenced by the sample preparation method [44]. The obtained values of parameter β in the tested sand samples are within the value range found in the literature.

Table 1. Empirical constants in the relationship between the degree of saturation and electrical resistivity according to Equation (4) [45].

Soil	Effective Size d_{50} [mm]	[-]	R^2 [-]
Fine sand (FSa)	0.22	1.63	0.93
Medium sand (MSa)	0.40	1.61	0.93
Coarse sand (CSa)	0.80	1.53	0.95

Figure 7a shows the relation between electrical resistivity and saturation degree of fine sand moistened with different KCl solutions. This graph shows how important the electrical conductivity of a fluid filling the pore space is, and what error can be made in in situ tests when trying to estimate the soil saturation degree when the electrical resistivity of this soil in fully saturated conditions is not known. In addition, this error can be greater at higher soil moisture contents [2].

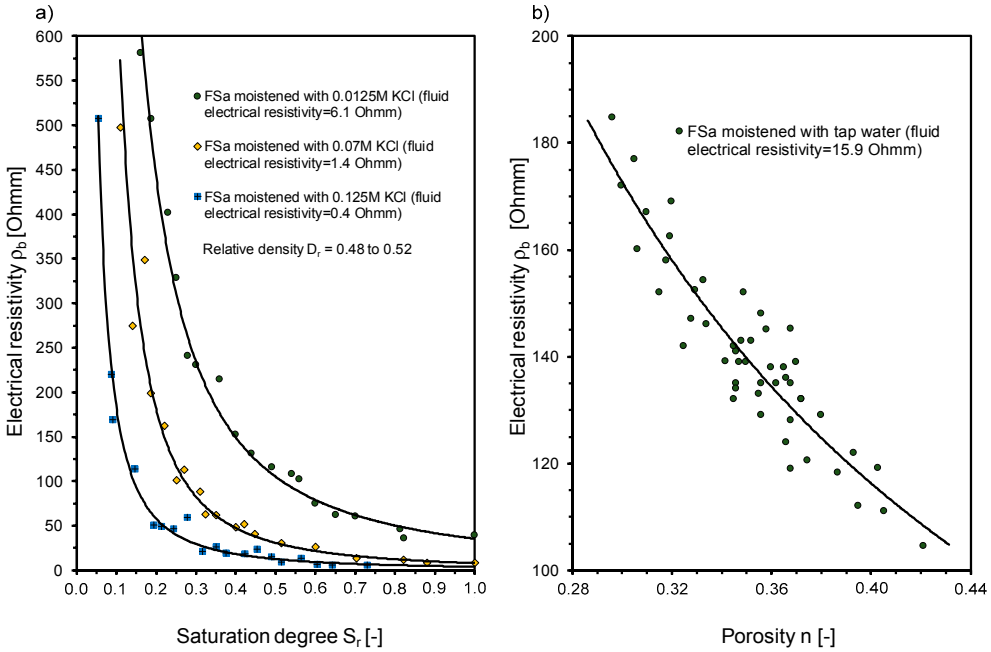

Figure 7. Analytical relation between electrical resistivity of fine sand (FSa) moistened with different KCl solution vs. saturation degree (**a**) and electrical resistivity vs. porosity (**b**).

To assess the effect of porosity on soil electrical resistivity, a number of tests were carried out on fully saturated sand samples compacted with a relative density (D_r) between 0.14 and 0.87. The empirical constants for use in Equation (5) are presented in Table 2, while Figure 7b shows an example of the relationship between electrical resistivity and porosity for fine sand.

$$n = \left(\frac{1}{F}\right)^{\frac{1}{m}} = \left(\frac{\rho_f}{\rho_{bSAT}}\right)^{\frac{1}{m}}, \quad (5)$$

where n is the porosity [-], F is the formation factor [-], ρ_f is the electrical resistivity of fluid in pore spaces [Ω·m], ρ_{bSAT} is the electrical resistivity of soil in fully saturated conditions [Ω·m], and m is the empirical constant.

Table 2. Empirical constants in the relationship between porosity and electrical resistivity according to Equation (5) [45].

Soil	Effective Size d_{50} [mm]	m [-]	R^2 [-]
Fine sand (FSa)	0.22	1.39	0.86
Medium sand (MSa)	0.40	1.41	0.89
Coarse sand (CSa)	0.80	1.45	0.91

For practical purposes, direct correlation between porosity and electrical resistivity is in common usage. It is assumed that the tortuosity value is equal to 1. Literature reports for clean sands give the values of the tortuosity coefficient and the cementation exponent at a = 1.0 and m = 1.3, respectively [12]. Recent research and considerations have allowed to extend the range of these parameters, e.g., [12,42,46]. However, it should be remembered that in the case of unsaturated materials, this relationship will be inversed and the increase in porosity will lead to increase in the electrical resistivity of a porous medium [2]. This should be taken into account when interpreting data from in situ measurements.

In the case of cohesive soils, including unsaturated ones, a simple predictable relationship between porosity and electrical resistivity cannot be expected. For this purpose, tests of unsaturated cohesive soil samples were carried out in a modified oedometer. The electrical response, caused by the change in the load of the soil sample, can be interpreted in terms of changes in porosity and fabric features such as pore tortuosity and particle alignment [16].

Figure 8 shows the consolidation curves in relation to curves of electrical resistivity changes as functions of time. The electrical resistivity of the sandy clay sample (sisaCl from SGGW Campus) recorded during the test is inversely proportional to the increasing vertical stress. This study resulted in setting an empirical relation between porosity and electrical resistivity, which is shown in Figure 9 and describes this relation when the saturation degree is close to 1, and is described by the equation:

$$n = 0.004 \cdot \rho_b + 0.309, \quad (6)$$

where n is the porosity [-] and ρ_b is the electrical resistivity of soil [Ω·m].

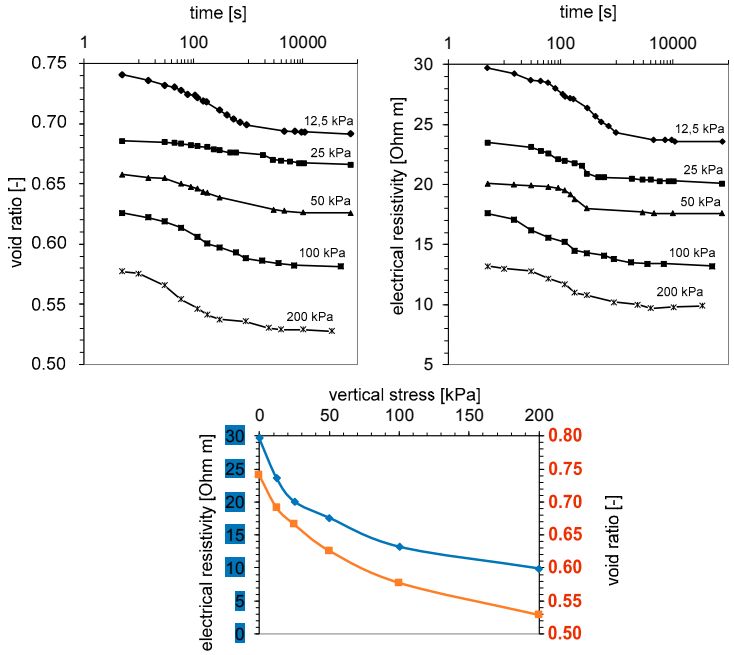

Figure 8. Changes in the void ratio and electrical resistivity during loading cycles of sandy clay (sisaCl) samples taken from the SGGW Campus in a modified oedometer.

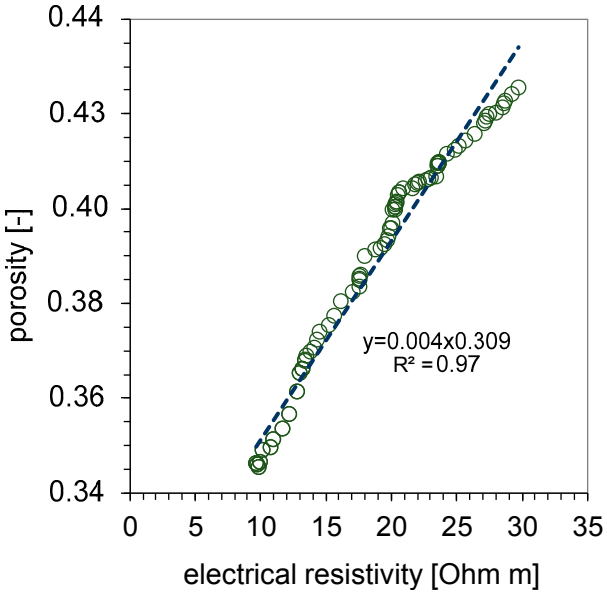

Figure 9. Analytical relation between electrical resistivity and porosity of sandy clay (sisaCl) based on oedemeter tests.

3.2. Assessment of Saturation Degree and Porosity—In Situ Investigations

The first example concerns the evaluation of porosity of Pliocene clays and sandy soils based on the resistivity cone penetration test (RCPT). Field studies require a slightly different approach than laboratory investigations; therefore, in order to set the porosity values as close as possible to real ones, the groundwater samples were taken from several depths and analyzed for variation of electrical conductivity. Values of electrical conductivity of groundwater taken using the BAT groundwater monitoring system [47] are presented in Table 3. Assuming that the saturation degree of clays is close to 1, the relationship between porosity and formation factor, F for clays in the tested site is as follows.

$$n = \left(\frac{1}{F}\right)^{\frac{1}{3.28}} = \left(\frac{\rho_f}{\rho_{bSAT}}\right)^{\frac{1}{3.28}} (R^2 = 0.79). \quad (7)$$

Assessment of porosity in cohesive soils is complicated and requires knowledge of the electrical resistivity of groundwater, which can vary with depth [30]. Electrical resistivity measurements assisted to geotechnical exploration in this case, and this simple relationship seems to be sufficient assuming that CEC and B+ are not included. Figure 10 shows the RCPT test results: changes in cone resistance q_c, friction ratio R_f, electrical resistivity profile and porosity calculated according to Equation (7). In addition, the figure presents the porosity values obtained from laboratory tests on undisturbed soil samples.

Table 3. Results of groundwater electrical conductivity measurements.

Depth [m]	Soil	Groundwater Conductivity [mS/m]
3.5	MSa	161.3
4.0	MSa	147.1
4.8	Cl	261.8
6.2	Cl	274.0
7.2	Cl	270.3
7.6	Cl	290.7
9.4	Cl	308.6
11.6	siCl	224.1

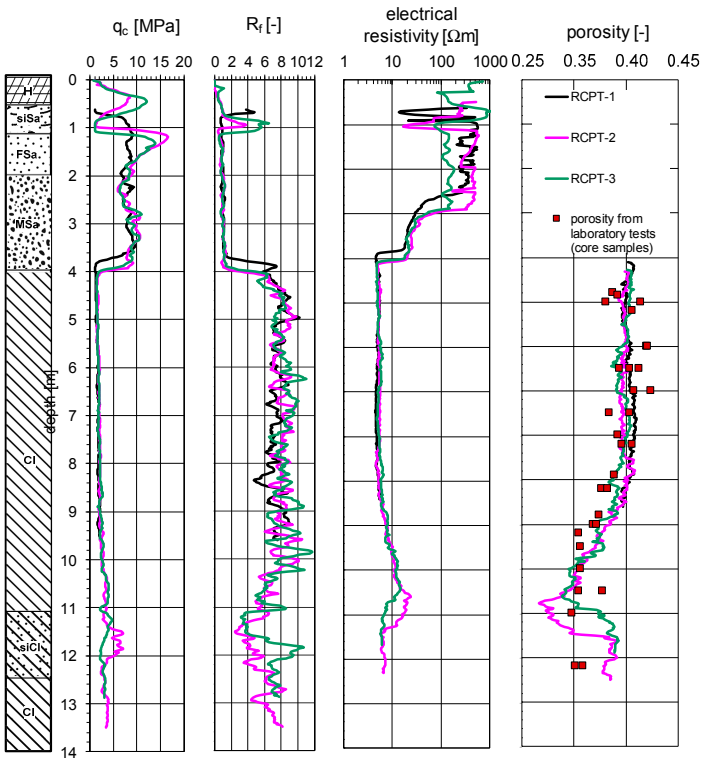

Figure 10. Results of RCPT tests; q_c—cone resistance, R_f—friction ratio, electrical conductivity and porosity of clays.

Figure 11 shows the distribution of the saturation degree of sands in the profile. The saturation degree values were calculated based on the Formula (4) and supplemented with the results of laboratory tests. The fully saturated zone starts from the depth of about 3.4 m below the surface; for this zone the porosity of sands was estimated according to Formula (5). Empirical constants appropriate for the given type of soil and proposed in Tables 1 and 2 were adopted in the calculations.

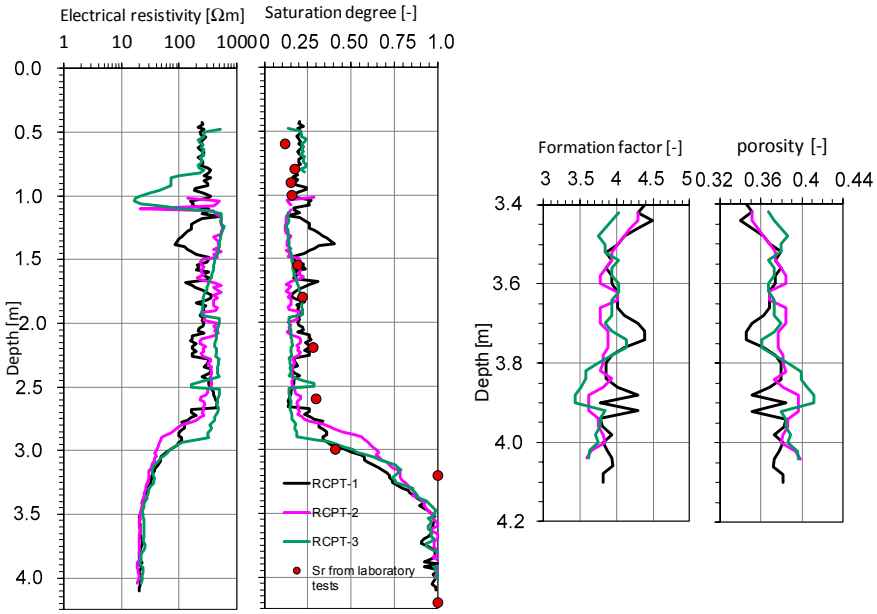

Figure 11. Results of RCPT tests; electrical resistivity of sands with calculated/measured saturation degree, formation factor and porosity of sands.

The next example presents the RCPT test with a calculated porosity of unsaturated sandy clay (sisaCl) at the SGGW Campus. An undisturbed soil sample was taken from the depth of about 5.5 m and compressed in a modified oedometer. This study allowed to establish a simple relationship between electrical resistivity and porosity presented in Figures 8 and 9. Figure 12 presents the RCPT test results with calculated porosity according to Equation (6). The porosity values in the top and bottom of the layer result from water penetration, which gives higher electrical conductivity in these zones and affects the obtained lower porosity values.

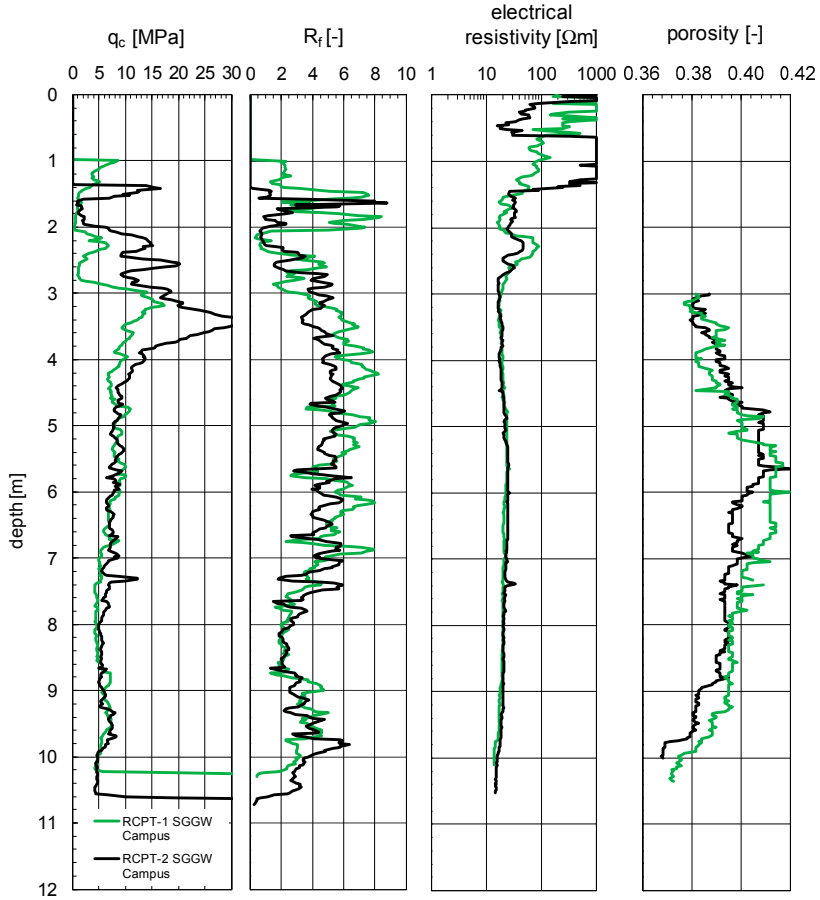

Figure 12. Results of RCPT tests; electrical resistivity of sands with calculated porosity of sandy clay.

Studying the relationship between porosity, saturation degree and electrical resistivity is interesting in both geophysics and geotechnics, e.g., [33,37]. The presented relationships showed a positive relation in these studies. However, electrical resistivity measurements still remain empirical and site restricted. The application of the above relationships in practice, and especially those used for cohesive soils, is only possible for a specific locality and soil type. Equations (4) and (5) established for sands seem to be universal and similar relationships were determined in other areas. The use of RCPT probes for this purpose is easier due to the measurement accuracy than the use of surface geophysical surveys.

3.3. Surface Resistivity Measurements—Recognition of Subsoil and Hydrotechnical Structures

Electrical resistivity methods are often applied to investigations of hydrotechnical structures because resistivity values obtained by these methods are very valuable for estimating the soil conditions of levees, e.g., [8,10,11]. Below are presented example results of surface surveys using electrical resistivity tomography (ERT) to detect weakened and damaged areas of the embankment body and its base, quality control of a vertical sealing system on a modernized levee, and recognition of the geological structure of a building foundation.

In the first case, the tests aimed to determine the condition of a selected section of the embankment, i.e., areas susceptible to dangerous filtration effects. The tests were performed on the Vistula river right-bank embankment. The area has been subject to numerous leakages through the embankment body and base. The embankment was 6 m high, the crest was 3 m wide, and the slope gradient was 1:1.7 to 1:2. The embankment fill is composed of fine sands with local inclusions of silt and silty clay, and the base is made of alluvial sands locally covered with a layer of flood deposits (Figure 13).

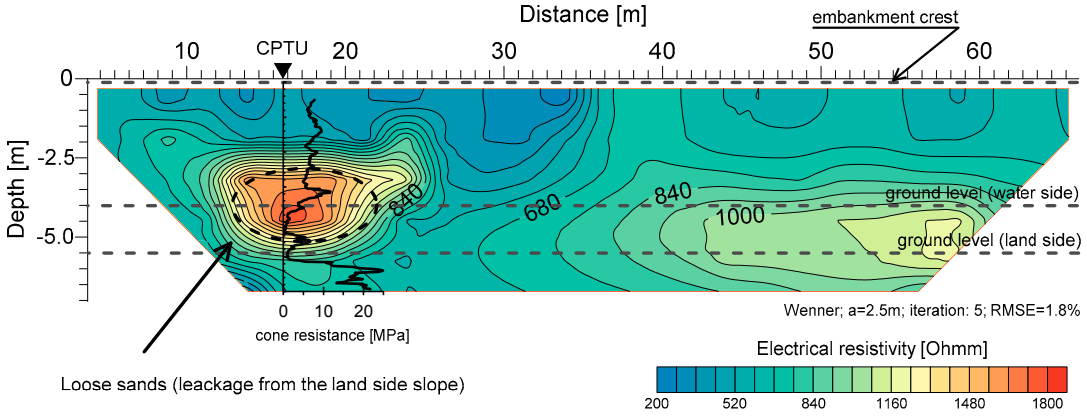

Figure 13. Geoelectrical cross-section through the embankment compared with cone resistance from the CPTU test.

Figure 13 shows the example results of electrical resistivity imaging. Along the entire length of the analyzed embankment section, the electrical resistivity of its fill was between 600 and 800 Ωm. The analysis included the embankment sections, in which electrical resistivity was significantly different from the background values (~600 Ωm). An area of significantly higher electrical resistivity up to 2000 Ωm was observed on the left side of the cross-section. High electrical resistivity may indicate loosened soil in this area and significant leakage through the embankment body. Control tests using a CPTU probe to validate the electrical resistivity results in this area indicate the presence of loosened soil.

The CPTU graph shows the decrease in the cone resistance (q_c) at the depth of 3.4 to 5.2 m. The cone resistance in this area was reduced from 6 to 2 MPa, while the friction ratio (R_f) did not change and varied between 1.2 and 1.6. The weakened zone in the embankment body is slightly different from the range defined on the basis of geophysical research. Despite these differences, geophysical surveys have indicated places for detailed geotechnical investigations with the CPTU probe. The results confirmed the need for modernization of this embankment section. In 2015, restoration works included construction of a vertical sealing system—DSM (Deep Soil Mixing) columns in the embankment body.

Geophysical surveys were conducted again; this time they were aimed at indicating the sealing continuity. The electrical resistivity method was used to distinguish the less permeable vertical layer in the embankment body. The purpose of the tests was also to investigate the depth of the DSM columns and confirm the sealing continuity. For a more accurate diagnosis, direct soundings could then be used [48]. The interpretation and testing results are presented in Figures 14 and 15.

In the figure below (Figure 14), the central part of the cross-section through the embankment body includes a zone with lower electrical resistivity, which is less than 50 Ωm. The left and right sections had electrical resistivity values of more than 160 Ωm (250 Ωm to the right), which indicates the occurrence of sandy deposits. A cross-section across the embankment (Figure 12) shows the presence of a hydraulic window. Electrical resistivity in the sealing zone is about 50 Ωm, while to the left (between 8 and 18 m of the cross-section), the values of electrical resistivity correspond to values in the embankment body.

In conclusion, geophysical surveys have not recorded the presence of sealing in this area, which gives the opportunity to evaluate the range of the problem and related detailed research on a given section of the embankment.

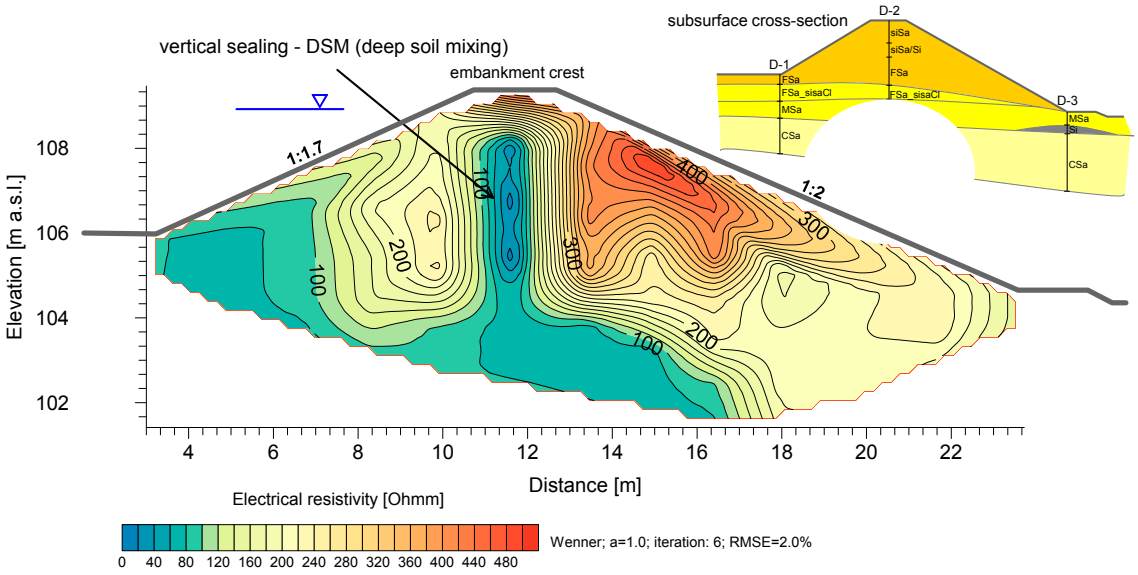

Figure 14. Geoelectrical cross-section across the embankment body after installing the sealing system.

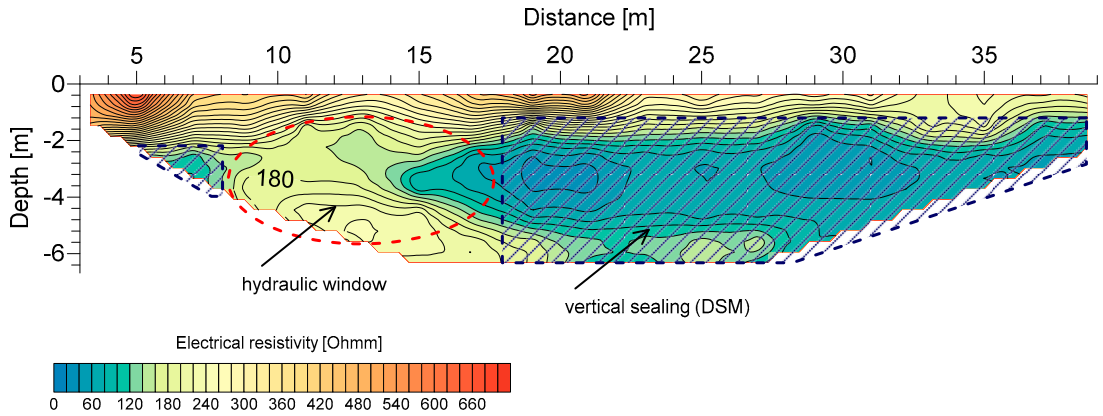

Figure 15. Geoelectrical cross-section across the embankment after installing the sealing system (view of vertical sealing and hydraulic window in the embankment body).

Similar observations were also made by other researchers [10] at a small earthen dam in Colorado where anomalous seepage was observed. The resistivity anomalies were used to delineate three seepage zones within the dam. Another example illustrates the resistivity investigations of a ground under an earth dam where the alluvial deposits, with resistivity reach 150 Ωm, overlay the resistive hard limestones bedrock (more than 1100 Ωm). The appearance of anomalies in geoelectrical cross sections indicates opened cavity filled with alluvial deposits (40 to 150 Wm). These discontinuities in the bedrock form additional possible pathways for water leakage from the dam reservoir [11]. The proposed approach could be easily practiced in other similar objects suffering from leakage's problems.

The next two examples include geophysical surveys, which were carried out in order to complete the geotechnical investigations. Previous research showed a high diversity of the geological structures; in particular the depth of the top of Pliocene deposits and its physical parameters in the analyzed area, e.g., [35,49]. The properties of these deposits determine the geotechnical design of the above ground and underground structures. These formations require a detailed analysis before their use as building foundation.

The first one—the Vistula slope area—shows the use of electrical resistivity measurements to determine the top of undisturbed clay deposits. For this purpose, several electrical resistivity profiles were carried out. Figure 16 shows a geoelectrical cross-section in combination with cone resistance qc and dilatometric index I_D values obtained during CPTU and DMT (flat dilatometer test) tests.

CPTU and DMT tests showed a diversified structure of the colluvial-delluvial deposits in the slope area. The change in cone resistance and dilatometric index indicates the top of clay deposits at 6 ÷ 6.5 m below ground level (DMT-2, CPTU-2) in the western and middle part of the cross-section. The cone resistance values obtained during CPT-3 testing (eastern part of the cross-section) showed diverse parameters and thus significant diversity of strength and strain parameters due to numerous lenses in colluvial-delluvial deposits in the slope area. Two zones: one at 7.5 to 11 m—cone resistance 1 ÷ 2 MPa (clay in the colluvial area) and one below 11 m—cone resistance of approximately 3 MPa, were observed during the analysis of cone resistance during CPT-3 testing. The difference in measured cone resistance indicates 11 m as the depth of the undisturbed top of clay deposits and the bottom of colluvial-delluvial deposits.

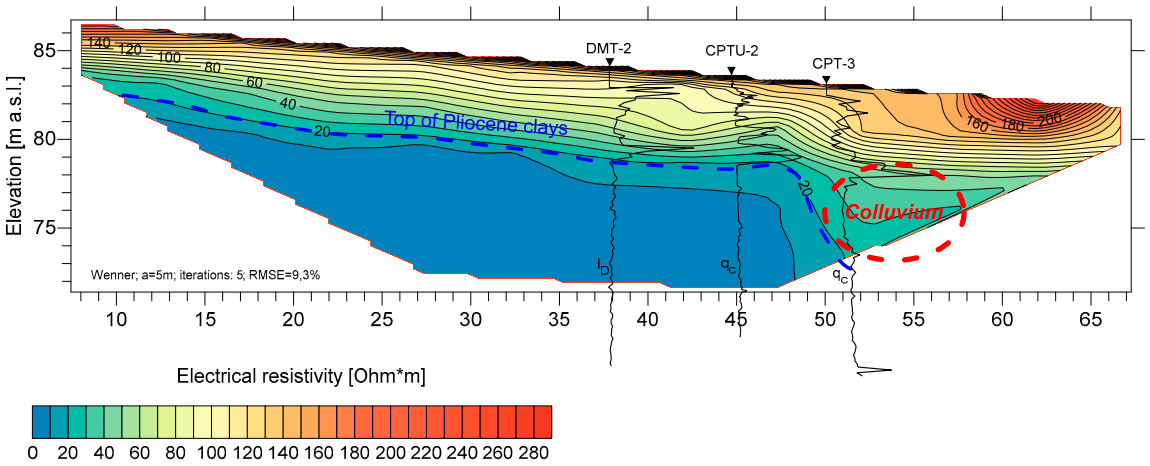

Figure 16. Geoelectrical cross-section in the Vistula slope area compared with cone resistance q_c from CPTU and material index from DMT tests.

High electrical resistivity up to 200 Ωm, specific for non-cohesive formations in the area can be observed in the electrical resistivity cross-section used in the analysis up to 2 m below ground level. With depth increase, the values decrease to several Ωm, which indicates the presence of cohesive soils. The decline in the resistivity isoline towards the east, corresponding to the terrain slope, can be observed on the right side of the cross-section.

Changes in electrical resistivity of the subsoil and their detailed analysis have allowed to determine the top surface of clay deposits, assuming that the boundary of the top of Pliocene deposits runs along the 20 Ωm isoline. The top of undisturbed Pliocene deposits is parallel to the terrain slope, and then declines rapidly (between 40 and 50 m of the profile) towards the Vistula River.

The second study shows the geoelectrical cross-section of the subsoil in the vicinity of water intake in one of the southern districts of Warsaw. The graph shows changes in electrical resistivity in the area to the depth of approximately 15 m below ground level (Figure 17). Analysis of the cross-section shows that non-cohesive soils with electrical resistivity of up to 200 Ωm occur at the depth of approximately 6 m. However, in the middle of the cross-section, the base of non-cohesive formations occurs at the depth of approximately 4.5 m, and in the areas planted with trees and shrubs it was determined at the depth of approximately 6 m based on changes of electrical resistivity. In this area, the layer of soils showing higher electrical resistivity reaches slightly deeper. This may be due to the lower moisture content of the soils in the rhizosphere, and thus the determined position of the base of sand in this area may be erroneous. The position of the top of clay deposits in this area must be validated by boreholes or probing. Soils characterized by resistivity of several to several dozen Ωm can be observed below the non-cohesive formations.

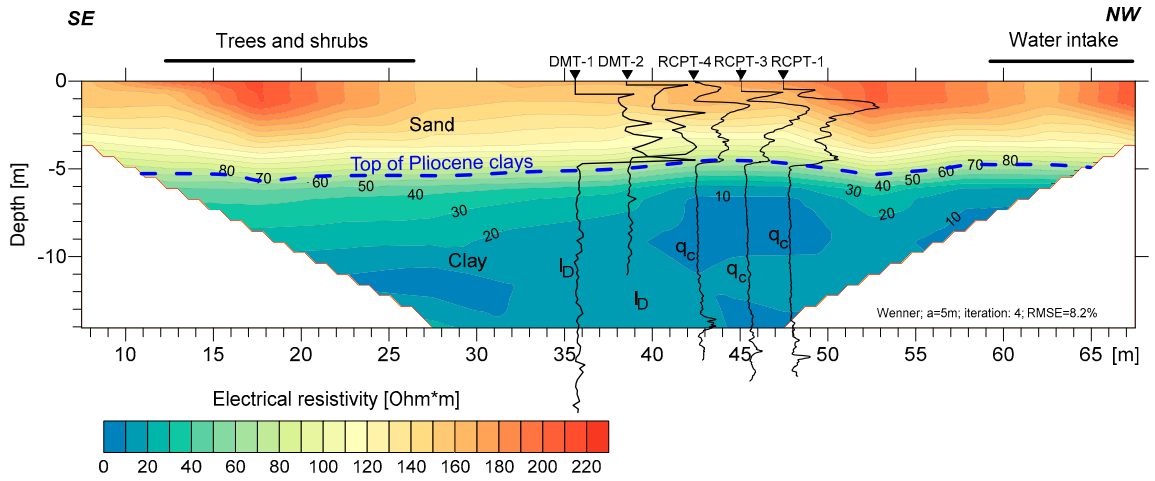

Figure 17. Geoelectrical cross-section of the Stegny site compared with the cone resistance q_c from CPTU and material index from DMT tests.

The cross-section also shows the cone resistance values (q_c) obtained during RCPT tests and the material index values (change in I_D value below 0.6 indicating transition into silty soil) obtained from DMT tests. Both the cone resistance and the material index show the transition in the soil type in the tested area at the depth of 4.0 ÷ 4.2 m below ground level. Detailed analysis of RCPT tests (Figure 10) shows a boundary between sands and clays in this area at the depth of approximately 4 m below ground level. The electrical resistivity for sands is between 100 Ωm to several hundred Ωm, and for clays between 4 Ωm and 12 Ωm.

The spatial data on changes in electrical resistivity from geophysical surveys and RCPT and DMT tests allowed for determining the top surface of clay deposits at the entire length of the profile. In a similar case, geophysical investigations, seismic surveys and geotechnical soundings were used to identify the top of cohesive soils in the area of an earth dam [50]. In the latter case, the value of 200 Ωm was found as a boundary between cohesive and non-cohesive formations. In addition, in geophysical studies, anomalies were identified and zones of soil loosening, which may have been caused by suffusion processes were distinguished.

4. Summary

The article presents some examples of electrical resistivity measurements in geotechnical and environmental investigations. Generally, electrical resistivity tests may be performed at a preliminary stage to determine the ground conditions or as supplementary tests for monitoring purposes. Surface geophysics allow for preliminary determination of the subsoil structure and indication of areas for detailed analysis using geotechnical probing (e.g., CPTU, RCPTU).

The presented laboratory tests have established some relationships between physical parameters and electrical resistivity in sands and clayey soils. When the soil sample is fully saturated, free of clay, and the pore water has a high salinity, the material is in good agreement with Archie's conditions. In such cases, determining the relationship between porosity and electrical resistivity will not cause problems, both in laboratory and field investigations. In the case of cohesive soils, it depends on the surface conductance effect and the interpretation of these data becomes more complex. The assessment of porosity on the basis of field tests requires an individual approach and the relations proposed in the paper are of regional nature. Geophysical investigations performed on selected sites have confirmed its usefulness when analyzing geological, hydrogeological and environmental conditions of the subsoil.

The studies have confirmed that electrical resistivity data can be used in quantitative analysis, e.g., to determine soil porosity and degree of saturation, however they require known conductivity values of pore water. While this is not a problem in sandy soils, in cohesive soils it requires the installation of specialized sampling equipment, e.g., BAT water monitoring systems. In specific cases, e.g., failure of

sealing systems in the embankment, non-standard methods are often required. However, each case should be analyzed separately due to the variety of factors affecting the results. The most important is the water content of the material. In fully saturated conditions, higher medium porosity will result in lower electrical resistivity in relation to the background. In an unsaturated medium, the relationship will be reverse, as it is the case in Figure 10, where differences in electrical resistivity allowed for determining the weakening zone in the embankment body.

It needs to be emphasized that a comprehensive interpretation of geophysical tests can only be conducted when reliable geological or geotechnical data supplemented with geochemical data sets are available. A complex interpretation of such data allows for appropriate design and monitoring of various engineering facilities.

Author Contributions: M.L., Z.S., M.B. and K.M.-L. conceived and designed the experiments; M.L., M.B. and Z.S. performed the experiments; M.L., Z.S., M.B. and K.M.-L. analyzed the data; M.L., Z.S., M.B. and K.M.-L. wrote the paper. All authors have read and agreed to the published version of the manuscript.

Funding: This research received no external funding.

Conflicts of Interest: The authors declare no conflict of interest. The founding sponsors had no role in the design of the study; in the collection, analyses, or interpretation of data; in the writing of the manuscript, and in the decision to publish the results.

References

1. Wisen, R.; Dahlin, T.; Auken, E. Resistivity imaging as a tool in shallow site investigation–a case study. In Proceedings of the 2nd International Conference on Site Characterization (ISC-2), Porto, Portugal, 20–22 September 2004; Viana de Fonseca & Mayne: Rotterdam, The Netherlands, 2004; pp. 607–613.
2. Reynolds, J.M. *An Introduction to Applied and Environmental Geophysics*; John Wiley and Sons Ltd.: New York, NY, USA, 2011.
3. Long, M.; Donohue, S.; L'Heureux, J.-S.; Solberg, I.-L.; Rønning, J.S.; Limacher, R.; O'Connor, P.; Sauvin, G.; Rømoen, M.; Lecomte, I. Relationship between electrical resistivity and basic geotechnical parameters for marine clays. *Can. Geotech. J.* **2012**, *49*, 1158–1168. [CrossRef]
4. Kowalczyk, S.; Zawrzykraj, P.; Mieszkowski, R. Application of electrical resistivity tomography in assessing complex soil conditions. *Geol. Q.* **2015**, *59*, 367–372. [CrossRef]
5. Zahody, A.A.P.; Eaton, G.P.; Mabey, D.R. Electrical methods in US Geological Survey. In *Ch. 2: Application of Surface Geophysics to Ground–Water Investigations*; USGS Publications: Reston, VA, USA, 1974.
6. Giang, N.V.; Duan, N.B.; Thanh, L.N.; Hida, N. Geophysical Techniques to Aquifer Locating and Monitoring for Industrial Zones in North Hanoi, Vietnam. *Acta Geophys.* **2013**, *61*, 1573–1597. [CrossRef]
7. Trappe, J.; Kneisel, C. Geophysical and Sedimentological Investigations of Peatlands for the Assessment of Lithology and Subsurface Water Pathways. *Geosciences* **2019**, *9*, 118. [CrossRef]
8. Stopiński, W. Bedrock monitoring by means of the electric resistivity method during the construction and operation of the Czorsztyn-Niedzica dam. *Acta Geophys. Pol.* **2003**, *51*, 215–256.
9. Niederleithinger, E.; Weller, A.; Lewis, R.; Stoetzner, U. Evaluation of geophysical techniques for river embankment investigation. In *Geotechnical and Geophysical Site Characterization–Huang and Mayne*; Taylor and Francis Group: Abingdon-on-Thames, UK, 2008; pp. 909–914.
10. Al-Fares, W.; Asfahani, J. Evaluation of the leakage origin in Abu Baara earthen dam using electrical resistivity tomography, northwestern Syria. *Geofis. Int.* **2018**, *57*, 223–237.
11. Ikard, S.J.; Revil, A.; Schmutz, M.; Karaoulis, M.; Jardani, A.; Mooney, M. Characterization of focused seepage through an earthfill dam using geoelectrical methods. *Ground Water* **2014**, *52*, 952–965. [CrossRef]
12. Archie, G.E. The electrical resistivity log as an aid in determining some reservoir characteristics. Transactions of the American Institute of Mining and Metallurgical Engineers. *Trans. AIME* **1942**, *146*, 54–61. [CrossRef]
13. Atkins, E.R.; Smith, G.H. The significance of particle shape in formation resistivity factor–porosity relationships. *J. Pet. Technol.* **1961**, *13*, 285–291. [CrossRef]
14. Jackson, P.D.; Taylor Smith, D.; Stanford, P.N. Resistivity–porosity–particle shape relationships for marine sands. *Geophysics* **1978**, *43*, 1250–1268. [CrossRef]

15. Abu-Hassanein, Z.S.; Benson, C.H.; Boltz, L.R. Electrical resistivity of compacted clays. *J. Geotech. Eng.* **1996**, *122*, 397–406. [CrossRef]
16. McCarter, W.J.; Blewett, J.; Chrisp, T.M.; Starss, G. Electrical property measurements using a modified hydraulic oedometer. *Can. Geotech. J.* **2006**, *42*, 655–662. [CrossRef]
17. Waxman, M.H.; Smits, L.J.M. Electrical Conductivities in Oil-Bearing Shaly Sands. *Soc. Pet. Eng. J.* **1968**, *8*, 107–122. [CrossRef]
18. Kalinski, R.J.; Kelly, W.E. Estimating Water Content of Soils from Electrical Resistivity. *Geotech. Test. J. ASTM* **1993**, *16*, 323–329.
19. Fukue, M.; Minato, T.; Matsumoto, M.; Horibe, H.; Taya, N. Use of a resistivity cone detecting contaminated soil layers. *Eng. Geol.* **2001**, *60*, 361–369. [CrossRef]
20. Rinaldi, V.A.; Cuestas, G.A. Ohmic Conductivity of Compacted Silty Clay. *J. Geotech. Environ. Eng.* **2002**, *128*, 824–835. [CrossRef]
21. Samouelian, A.; Cousin, I.; Tabbagh, A.; Bruand, A.; Richard, G. Electrical resistivity survey in soil science. *Soil Tillage Res.* **2005**, *83*, 173–193. [CrossRef]
22. Batayneh, A.T. 2D electrical imaging of an LNAPL contamination, Al Amiriya Fuel Station, Jordan. *J. Appl. Sci.* **2005**, *5*, 52–59.
23. Mondelli, G.; Giacheti, H.L.; Elis, V.R. The use of resistivity for detecting MSW contamination plumes in a tropical soil site. In Proceedings of the 6th International Congress on Environmental Geotechnics, New Delhi, India, 8–12 November 2010; Mc Graw Hill: New York, NY, USA, 2010; pp. 1544–1549.
24. De Carlo, L.; Perri, M.T.; Caputo, M.C.; Deiana, R.; Vurro, M.; Cassiani, G. Characterization of a dismissed landfill via electrical resistivity tomography and mise-à-la-masse method. *J. Appl. Geophys.* **2013**, *98*, 1–10. [CrossRef]
25. Lech, M.; Fronczyk, J.; Radziemska, M.; Sieczka, A.; Garbulewski, K.; Koda, E.; Lechowicz, Z. Monitoring of total dissolved solids on agricultural lands using electrical conductivity measurements. *Appl. Ecol. Environ. Res.* **2016**, *14*, 285–295. [CrossRef]
26. Koda, E.; Tkaczyk, A.; Lech, M.; Osinski, P. Application of Electrical Resistivity Data Sets for the Evaluation of the Pollution Concentration Level within Landfill Subsoil. *Appl. Sci.* **2017**, *7*, 262. [CrossRef]
27. Friedman, S.P. Soil properties influencing apparent electrical conductivity: A review. *Comput. Electron. Agric.* **2005**, *46*, 45–70. [CrossRef]
28. Asfahani, J.; Zakhem, B.A. Geoelectrical and hydrochemical investigations for characterizing the salt water intrusion in the Khanasser valley, northern Syria. *Acta Geophys.* **2013**, *61*, 422–444. [CrossRef]
29. Greggio, N.; Giambastiani, B.M.S.; Balugani, E.; Amaini, C.; Antonellini, M. High-Resolution Electrical Resistivity Tomography (ERT) to Characterize the Spatial Extension of Freshwater Lenses in a Salinized Coastal Aquifer. *Water* **2018**, *10*, 1067. [CrossRef]
30. Campanella, R.G.; Weemees, I. Development and use of an electrical resistivity cone for groundwater contamination studies. *Can. Geotech. J.* **1990**, *27*, 557–567. [CrossRef]
31. Rice, A. The Seismic Cone Penetrometer. Master's Thesis, Department of Civil Engineering, University of British Columbia, Vancouver, BC, Canada, 1984.
32. Robertson, P.K.; Campanella, R.G.; Gillespie, D.; Greig, J. Use of Piezometer Cone Data. In Proceedings of the American Society of Civil. Engineers, ASCE, In-Situ 86 Specialty Conference, New York, NY, USA, 23–25 June 1986; pp. 1263–1280.
33. Kowalczyk, S.; Zawrzykraj, P.; Maślakowski, M. Application of the electrical resistivity method in assessing soil for the foundation of bridge structures: A case study from the Warsaw environs, Poland. *Acta Geodyn. Geomater.* **2017**, *14*, 221–234. [CrossRef]
34. Dahlin, T.; Garin, H.; Palm, M. *Combined Resistivity Imaging and RCPT for Geotechnical Preinvestigation*; Procs NGM: Ystad, Sweden, 2004; pp. 1–9.
35. Skutnik, Z.; Bajda, M.; Lech, M. *Applications of RCPTU and SCPTU with Other Geophysical Test Methods in Geotechnical Practice*; Hicks, M., Pisanò, F., Peuchen, J., Eds.; RC Press: London, UK, 2018.
36. Rabarijoely, S. A New Approach to the Determination of Mineral and Organic Soil Types Based on Dilatometer Tests (DMT). *Appl. Sci.* **2018**, *8*, 2249. [CrossRef]

37. Chu, Y.; Liu, S.; Cai, G.; Bian, H. Evaluation of Free Swelling of Expansive Soil Using Four-Electrode Resistivity Cone. In Proceedings of the China-Europe Conference on Geotechnical Engineering, Springer Series in Geomechanics and Geoengineering, Vienna, Austria, 13–16 August 2018; Wu, W., Yu, H.S., Eds.; Springer: Berlin/Heidelberg, Germany, 2018; pp. 685–688.
38. Lowrie, W. *Fundamentals of Geophysics*, 2nd ed.; Cambridge University Press: Cambridge, UK, 2014.
39. Pfannkuch, H.O. On the correlation of electrical conductivity properties of porous system with viscous flow transport coefficients. In Proceedings of the IAHR First International Symposium on Fundamentals of Transport Phenomena in Porous Media, Haifa, Israel, 23–28 February 1969; pp. 37–47.
40. Loke, M.H.; Chambers, J.E.; Rucker, D.F.; Kuras, O.; Wilkinson, P.B. Recent developments in the direct-current geoelectrical imaging method. *J. Appl. Geophys.* **2013**, *95*, 135–158. [CrossRef]
41. Keller, G.V.; Frischknecht, F.C. *Electrical Methods in Geophysical Prospecting*; Pergamon Press: Oxford, UK, 1966.
42. Buryakovsky, L.A. *Petrophysics: Fundamentals of the Petrophysics of Oil and Gas Reservoirs*; Scrivener Publication: Beverly, MA, USA, 2012.
43. Bahuguna, R.M.; Pabla, S.S.; Lal, M.; Raj, H. Impact on Estimation of Water Saturation Values Using Laboratory Determined 'a', 'm'& 'n' Parameters-A Case Study. In Proceedings of the 6th International Conference & Exposition on Petroleum Geophysics, Kolkata, India, 4–6 December 2006.
44. Schön, J. *Physical Properties of Rocks: A Workbook*; Elsevier: San Diego, CA, USA, 2011.
45. Lech, M. The Use of Electrical Resistivity Method to Recognize Ground Water Flow Conditions. Ph.D. Thesis, Department of Geotechnical Engineering, Warsaw University of Life Sciences, Warsaw, Poland, 2006. (In Polish)
46. Nabawy, B.S. Impacts of the pore- and petro-fabrics on porosity exponent and lithology factor of Archie's equation for carbonate rocks. *J. Afr. Earth Sci.* **2015**, *108*, 101–114. [CrossRef]
47. Torstensson, B.A. A new system for Groundwater Monitoring. Groundwater Monitoring Review. *Groundw. Monit. Remediat.* **1984**, *4*, 131–138. [CrossRef]
48. Skutnik, Z.; Bajda, M.; Lech, M. The selection of sealing technologies of the subsoil and hydrotechnical structures and quality assurance. *Open Eng.* **2020**, *9*, 420–427. [CrossRef]
49. Wójcik, E.; Trzciński, J.; Łądkiewicz-Krochmal, K. Microstructural changes of expansive clays during dehydration caused by suction pressure—A case study of Miocene to Pliocene clays from Warsaw (Poland). *Acta Geol. Pol.* **2019**, *69*, 465–488.
50. Mieszkowski, R.; Kowalczyk, S.; Barański, M.; Szczepański, T. The use of geophysical methods to identify the roof of cohesive soils and the designation of zones of suffusion relaxation in the body of an earth dam. (in Polish). *Zeszyty Nauk. Inst. Gospod. Surowcami Miner. Energią PAN* **2014**, *86*, 167–180.